ELSEVIER

Journal of Neuroscience Methods 60 (1995) 49–60

JOURNAL OF NEUROSCIENCE METHODS

Simultaneous optical recording of evoked and spontaneous transients of membrane potential and intracellular calcium concentration with high spatio-temporal resolution

Saurabh R. Sinha, Saumil S. Patel, Peter Saggau *

Division of Neuroscience, Baylor College of Medicine, Houston, TX 77030, USA

Received 20 June 1994; revised 4 November 1994; accepted 14 November 1994

Abstract

We have developed a system for simultaneous optical recording of transients of membrane potential and intracellular calcium concentration from mammalian brain slice preparations with high spatio-temporal resolution. Simultaneous recording was achieved by using two dedicated photodetectors together with two fluorescent indicators. Specifically, the calcium-sensitive dye Calcium Orange and the voltage-sensitive dye RH-414 were selected because they have overlapping excitation spectra, but separable emission spectra. Transverse guinea pig hippocampal slices were double-loaded by bath application of the membrane-permeant form of Calcium Orange and RH-414. Transients of intracellular calcium concentration and membrane potential associated with evoked neural activity in hippocampal areas CA1 and CA3 were recorded. Furthermore, we have recorded calcium and voltage transients associated with spontaneous epileptiform activity induced by bath application of an epileptogenic drug, 4-aminopyridine. The use of photodiode matrices (10 × 10 elements each) as detectors gives the high spatial (200 × 200 μm/element with a 10 × objective) and temporal resolution (570 μs/frame). The recording system also includes a CCD camera for obtaining images of the preparation and overlaying the image with the optically detected signals. A software package has been developed for setting up the experimental protocol(s) and for collecting, processing, displaying, and analyzing the data in an user-friendly, windows-based environment.

Keywords: Epileptiform activity; Fluorescence imaging; Membrane potential; Intracellular calcium; Brain slice; Voltage-sensitive dye; RH-414; Calcium indicator; Calcium Orange; Simultaneous recording

1. Introduction

Optical recording provides a means for measuring parameters of cellular activity such as ion concentrations and membrane potential transients with high spatial resolution. This technique also allows recording from sites inaccessible to more conventional approaches. In the case of ion concentration, it provides higher temporal resolution than conventional methods, such as ion-sensitive microelectrodes. Because of the physiological importance of intracellular calcium concentration ($[Ca^{2+}]_i$) and membrane potential (V_m), measurements of these parameters with calcium-sensitive dyes (CaSDs) and voltage-sensitive dyes (VSDs), respectively, are by far the most common applications of optical recording. Due to the complex interaction between these 2 parameters, there is great interest in measuring both together. In the case of spontaneous neural activity, such as spontaneous epileptiform activity (SEA), which is quite variable from event to event, these quantities must be measured simultaneously if correlations are to be drawn between them. Since the time course of neural activity is relatively fast, these signals must be measured with a high temporal resolution. Furthermore, because the spatial spread of such events is often of interest, sufficient spatial resolution is also required.

Many groups have optically recorded 2 parameters from the same preparation either by altering their apparatus between measurements of the 2 parameters or by making use of equipment and techniques developed for ratiometric measurement of a single indicator. Saggau and Sheridan (1990) alternately recorded transients of V_m and $[Ca^{2+}]_i$ from hippocampal brain slices double-loaded with the calcium indicator fura-2 and the VSD RH-414. Kremer et al. (1992) recorded $[Ca^{2+}]_i$ and V_m, using the CaSD indo-1 and the VSD bis-oxonol, with a fluorescence spectrophotometer equipped with

* Corresponding author. Fax: (713) 798-3946.

SSDI 0165-0270(94)00219-3

two pairs of excitation and emission monochromators. Since this experiment was performed on cell suspensions in a cuvette, the technique lacked spatial resolution. The parameters were measured alternately, using a light chopper, rather than truly simultaneously. The temporal resolution was only 500 ms. Martinez-Zaguillan et al. (1991), also using a fluorescence spectrophotometer and a light chopper, recorded pH and $[Ca^{2+}]_i$ using the pH-sensitive dye (pHSD) SNARF-1 and the calcium indicator fura-2 with a temporal resolution of 4 Hz. Tepikin et al. (1992) utilized a similar strategy (alternating between 2 excitation wavelengths) to record intracellular and extracellular calcium concentrations using the CaSDs fura-2 and fluo-3; the temporal resolution was on the order of several seconds. Employing a system where the excitation filters were located on a rotating filter wheel, Zorec et al. (1993) recorded intracellular pH and $[Ca^{2+}]_i$ with the pHSD BCECF and the CaSD fura-2. Their theoretical temporal resolution was near 8 Hz; however, due to the need for temporal averaging, the actual resolution was less than 2 Hz. Although they did not take advantage of it, their system did have spatial resolution. Miyata et al. (1989) performed a very similar measurement with the same 2 indicators with spatial resolution but without attempting to measure temporal aspects of the signals. The only previous report of truly simultaneous measurement of 2 parameters is the measurement of $[Ca^{2+}]_i$ and pH by Morris (1992). Using a 4-channel video microscope and the indicators indo-1 and SNARF-1, calcium and pH were measured with both spatial and temporal resolution. The temporal resolution of this system was limited to less than 60 frames/s; moreover, for most experiments, it was necessary to average 2–16 frames, reducing the temporal resolution even further. Thus, previous attempts at simultaneous optical recording of 2 parameters of cellular activity have been severely limited in spatial resolution, temporal resolution and/or sensitivity. Certainly none of them even approach the requirements for recording the signals we wish to record, i.e., transients of $[Ca^{2+}]_i$ and V_m associated with spontaneous neural activity.

In our strategy, simultaneous recording of both signals is achieved by using a CaSD, Calcium Orange, and a VSD, RH-414 (both from Molecular Probes, Eugene, OR), which have overlapping excitation spectra but distinct emission spectra (see Fig. 1). The peaks of the excitation spectra are 554 nm for Calcium Orange and 531 nm for RH-414; the peaks of the emission spectra are 575 nm for Calcium Orange and 714 nm for RH-414 (Haugland, 1992). These characteristics allow for simultaneous measurement without the need for switching between sets of filters, which would be inherently slower and a possible source of mechanical noise.

The 2 types of spatially resolving photodetectors amenable to conventional (non-scanning) microscopy

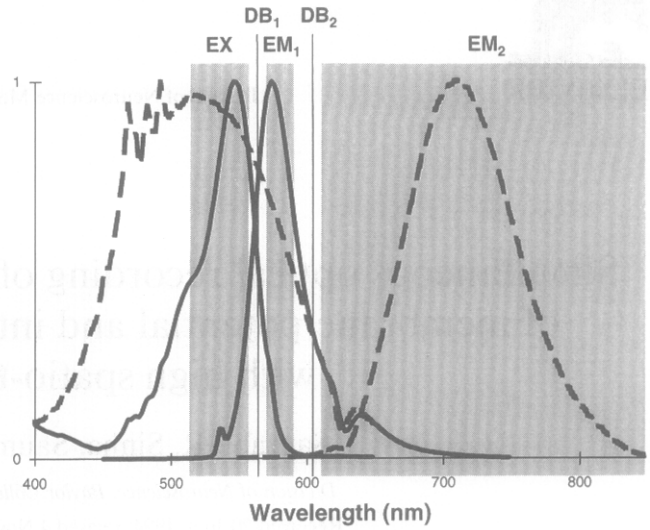

Fig. 1. Normalized excitation and emission spectra of Calcium Orange (solid lines) and RH-414 (dashed lines) and approximate characteristics of the employed excitation (EX) and emission filters (EM_1 and EM_2) and dichroic beamsplitters (DB_1 and DB_2). The 2 spectra on the left are the excitation spectra; the emission spectra are on the right. The indicators were dissolved in methanol (RH-414) or water (Calcium Orange) and the spectra measured with 2 nm resolution and 1 s integration time on a spectrofluorometer (SLM 8000, SLM Instrument). For the filters, the shaded boxes indicate the FWHM; note that because EM_2 is a longpass filter, its transmission continues past the edge of the graph.

applications are the CCD camera and the photodiode matrix (PDM). CCD cameras have the advantages of high spatial resolution (several hundred pixels in each dimension) and the capabilities of spatial and temporal integration on the detector chip. These integration capabilities make CCD cameras specially useful in low light applications; however, due to their mainly serial readout scheme, their temporal resolution only approaches a few hundred frames/s even with substantial spatial integration (Lasser-Ross et al., 1991; Patel and Saggau, unpublished results). In practice, the temporal resolution is even lower due to temporal integration, which is necessitated by the relatively low sensitivity to light (quantum efficiency) of a CCD camera. In contrast to CCD cameras, PDMs like single photodiodes have a relatively high quantum efficiency. Moreover, due their truly parallel readout scheme, they are also capable of very high temporal resolutions, usually limited by the amount of light and by the speed of the data acquisition and storage apparatus. Because of our requirement of high temporal resolution without the possibility of signal averaging (for spontaneous events) as well as spatial resolution, we used PDMs to record both types of optical signals.

After the initial use of fluorescent VSDs to record from hippocampal brain slices (Saggau et al., 1986), a PDM (Grinvald et al., 1981) was used to obtain spatial resolution (Saggau and Tenbruggencate, 1988). Since then, several groups have used this technique to record

evoked activity with high spatial and temporal resolution in brain slices (Albowitz et al., 1990) and various other preparations (Cinelli and Kauer, 1992; Fromherz and Vetter, 1992; Fukunishi et al., 1992; Litaudon and Cattarelli, 1992). More recently, this technique has been extended to recording SEA in transverse hippocampal slices (Colom and Saggau, 1994). Signals from fluorescent CaSDs in response to evoked activity have mostly been recorded using either single photodiodes, which provide no spatial resolution when used with conventional microscopes, or CCD cameras. Ross et al. (1988) did employ a PDM to record calcium transients from cultured leech neurons with the absorbent calcium indicator arsenazo III. Hess and Kuhnt (1992) used a PDM with the fluorescent CaSD Calcium Green to record evoked calcium transients from hippocampal slices; however, the spatial characteristics of these signals were not reported. The only report of using CaSDs to measure signals due to spontaneous neural activity is the imaging of calcium in dendrites of cultured cortical neurons in response to quantal synaptic transmission by Murphy et al. (1994).

In this paper we describe the hardware, software and protocols we have developed to simultaneously record membrane potential and intracellular calcium transients with high spatial and temporal resolution. We will also describe the application of this method to record transients associated with evoked and spontaneous activity in transverse brain slices from the guinea pig hippocampus. Finally, we will discuss possible refinements and modifications to the loading technique and hardware.

2. Materials and Methods

2.1. Apparatus

Fig. 1 shows the excitation and emission spectra of Calcium Orange and RH-414 in solution (see figure legend) along with the approximate spectral character-

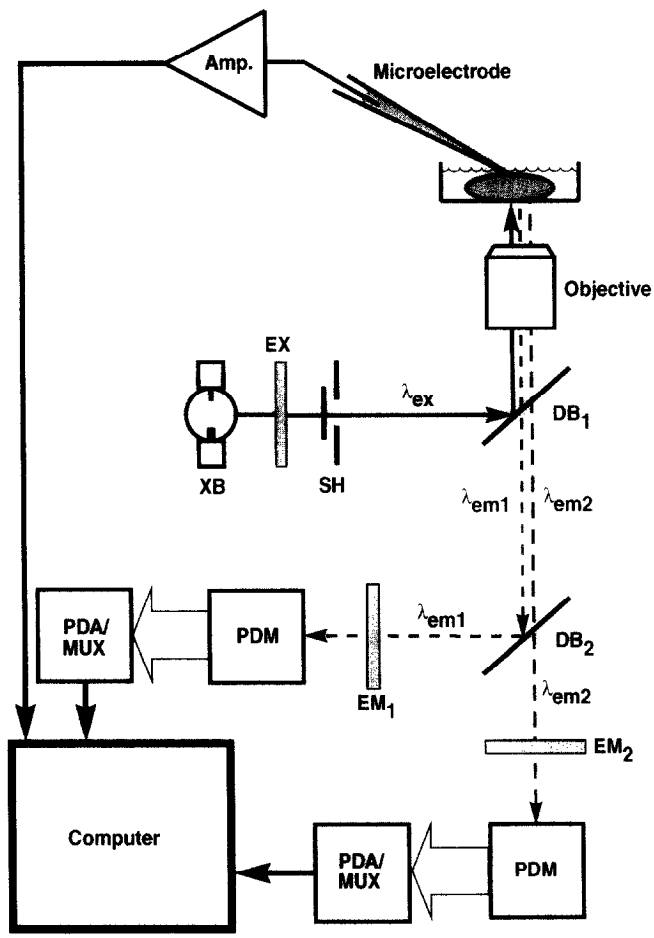

Fig. 2. Schematic of the optical recording setup. The excitation light is produced by a xenon burner (XB), and passes through the excitation filter (EX) and a computer-controlled shutter (SH). The first dichroic beamsplitter (DB_1) directs the excitation light (λ_{ex}) onto the preparation through the objective and collects the emitted fluorescence (λ_{em}) from the preparation and sends it to the remainder of the apparatus. The second dichroic beamsplitter (DB_2) separates the fluorescence into 2 components corresponding to each indicator (λ_{em1} for Calcium Orange, λ_{em2} for RH-414). Each component passes through an appropriate emission filter (EM_1 or EM_2) and onto a dedicated photodiode matrix (PDM_1 or PDM_2). The signals from the PDM are current-to-voltage converted, amplified, filtered and multiplexed by the photodiode amplifiers (PDA/MUX) and sent to the computer. A microelectrode is used to record the field potential.

istics of the filters and dichroic beamsplitters used to excite the indicators or to separate their fluorescence. The measured peaks of the spectra were very close to the literature values (Haugland, 1992): for RH-414, 518 nm excitation and 708 nm emission; for Calcium Orange, 548 nm excitation and 574 nm emission. The large overlap between the excitation spectra of the 2 indicators allows one to use a single excitation filter (EX, 535/45 nm: 535 nm center wavelength and 45 nm full width at half maximum transmission, FWHM) to excite both. The first dichroic beamsplitter (DB_1, 565 nm cut-on wavelength) separates the excitation light from the fluorescence emitted by the 2 indicators. A second dichroic beamsplitter (DB_2, 605 nm cut-on wavelength) separates this fluorescence into 2 components corresponding to the emission spectra of the 2 dyes. The 2 emission filters further improve the separation of the fluorescence components: EM_1 (580/20 nm) for Calcium Orange and EM_2 (610 nm longpass) for RH-414. All dichroic mirrors and filters were obtained from Omega (Brattleboro, VT). The slight overlap in the emission spectra of the 2 indicators makes complete optical separation of the 2 fluorescence signals difficult. This is exacerbated by the true characteristics of the emission filters and DB_2. The FWHM of a filter indicates the window of wavelengths within which the filter transmits more than 50% of its maximum transmission; and, while the transmission declines relatively steeply on either side of the window, a small but significant amount of light at wavelengths outside this window is transmitted by the filter. This problem of incomplete separation was addressed by a data processing method (see below).

Fig. 2 shows schematically how these filters and mirrors are used. The setup is based on an inverted microscope (IM35, Zeiss; not shown in figure). The excitation light is provided by a 75 W xenon burner (XB; XBO 75W/2, Osram) supplied by a constant current source, which draws its power from a bank of batteries for improved stability. Light passes through the excitation filter (EX) and a computer-controlled shutter (SH, Uniblitz, Vincent, Rochester, NY). The first dichroic beamsplitter (DB_1) is used to reflect the excitation beam onto the stained preparation and to transmit the fluorescence from the preparation towards the detectors. The second dichroic beamsplitter (DB_2) and the 2 emission filters (EM_1 for Calcium Orange and EM_2 for RH-414) are located in the light path to the PDMs (MD-100 Centronics, Newbury Park, CA). Both PDMs are located in corresponding image planes of the microscope.

DB_2 is located in a slider, which contains a mirror in its second slot (not shown). When this mirror is in place, light from the preparation is reflected onto a CCD camera. When used with transillumination, the CCD camera obtains an image of the preparation. The transillumination is at wavelengths greater than 630 nm in order to avoid bleaching of the dyes. The CCD image is captured by a 640×480 pixel, 8-bit, RS-170 interface frame grabber (IP-8/AT, Matrox, Dorval, Canada) which also allows for overlaying of the optical signals on the CCD image. Routinely, the CCD image is aligned with the 2 PDMs, such that corresponding elements of the 2 PDMs coincide with each other and with a 10×10 grid superimposed on the CCD image. This grid and the captured CCD image can then be used to determine the exact location on the preparation from which a particular signal was recorded.

The signals from the PDMs are current-to-voltage onverted, filtered, and amplified by the photodiode

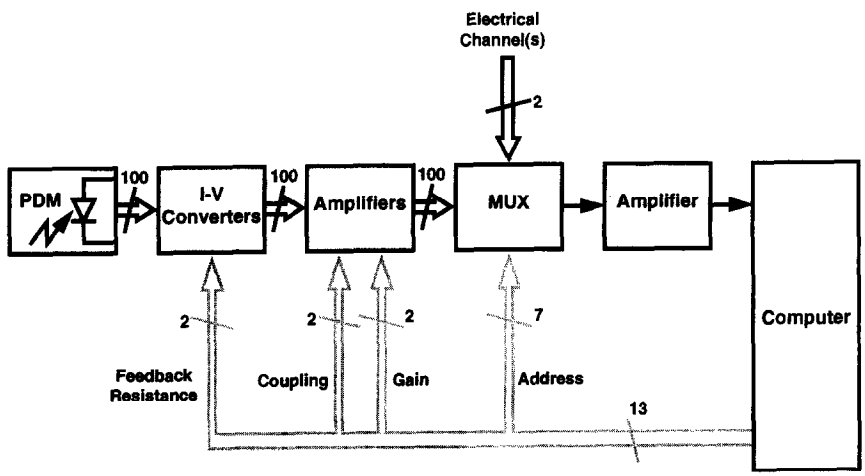

Fig. 3. Schematic of the PDAs and the digital control lines from the computer. The currents from all 100 elements of each PDM are sent to the PDA, which consists of two 100-channel stages: a current-to-voltage converter (I-V converter) and an amplifier. The output of the amplifier is multiplexed (MUX) along with 2 additional electrical channels (one was used for the field potential). A single-channel amplifier is located after the MUX; the output from this amplifier is sent to the computer for digitization, demultiplexing, display, storage, and analysis. Thirteen digital lines from the computer are used to control various aspects of the PDA and MUX: 7 lines for the MUX address, 2 lines to control the feedback resistance of the I-V converters, and 2 lines each to control the coupling type and gain of the second stage.

amplifiers (PDAs). Each PDA contains 100 dual-stage amplifiers (one for each element of the matrix). As shown in Fig. 3, each PDA receives digital lines from the computer (486/50; IBM clone) which control: (1) the feedback resistor of the current-to-voltage converter (1, 10, or 100 MΩ), (2) the type of coupling between the first and second stage (DC; fast AC, 10 ms settling time constant; or slow AC, 100 ms settling time constant) and (3) the gain of the second stage (1, 10, 1000, or 5000). In addition, each PDA receives a 7-bit multiplexer (MUX) address which is generated from a counter driven by the element clock (half the sampling clock rate). The PDAs are also capable of multiplexing 2 external analog inputs with the optical data. A final amplification stage (manually controlled gain: 1, 2, 5, or 10) is located after the multiplexer stage.

A multipurpose I/O card (Flash-12, Strawberry Tree, Sunnyvale, CA) is used for A/D, D/A and digital I/O. The specifications for this card are, A/D converter: 8 channels, 12-bit, 400 kHz with 256 ksample on-board memory; D/A converter: 2 channels, 12-bit, 400 kHz with 256 ksample on-board memory; and digital I/O: 8 lines, TTL. Two channels of the A/D converter are employed for the multiplexed PDM signals. The D/A converters are used for stimulation. The TTL I/O lines along with 8 more digital output lines from the parallel printer port are used for multiplexer addressing and controlling the shutter and the PDA.

2.2. Software

A software package (Patel et al., 1993) has been developed to set up the experimental protocol(s) and to collect, process, display and store the data in a windows-based environment (Microsoft). It allows concurrent data collection from a variety of analog sources (conventional electrodes, single photodiodes, PDMs, and video cameras). It also generates the required analog (stimulation) and digital (control and addressing) signals. The configuration of these analog and digital events along with other data collection parameters (timing, collection mode, etc.) is interactively entered by the user. The data can be monitored on-line, with each PDM element individually displayed as a 2-dimensional array overlaid on the image of the preparation, and as the average of all matrix elements. Clusters of PDM elements can also be interactively set up and the optical signals displayed as the average of the signals from all elements within a cluster. For off-line analysis, the data can be converted to ASCII files and processed (see below) using third party software.

2.3. Preparation and solutions

Transverse hippocampal slices were prepared by standard methods from guinea pigs (male, wild-type, 100–150 g). The animals were anesthetized (methoxyflurane) and quickly decapitated. Brain slices were prepared from the middle third of the hippocampus on a vibrating tissue cutter (Vibratome 1000, TPI) and were stored in artificial cerebro-spinal fluid (ACSF) containing: 124 mM NaCl, 5 mM KCl, 2 mM $CaCl_2$, 1.2 mM $MgCl_2$, 26 mM $NaHCO_3$, and 10 mM D-glucose. The ACSF was saturated with 95% O_2/5% CO_2 to maintain a constant pH of 7.4. Spontaneous epileptiform activity was induced by adding 4-aminopyridine (4-AP, 100 μM) to the ACSF.

2.4. Loading

Slices were sequentially loaded with Calcium Orange and RH-414. All staining or holding salines were either bubbled with 95% O_2/5% CO_2 or had this gas mixture blown over them. The membrane-permeable acetoxymethyl ester (AM) of Calcium Orange (50 μg) was dissolved in 10 μl DMSO containing 25% (w/w) pluronic acid (F-127, BASF Wyandotte, obtained from Molecular Probes, Eugene, OR), a detergent. ACSF (1 ml) was added to the dissolved Calcium Orange-AM, giving final concentrations of 40 μM Calcium Orange-AM, 0.75% DMSO and 0.25% pluronic acid. This solution was sonicated for 10 min; and then transferred to a 35 mm petri dish which was placed in a 30°C water bath. Five to 7 slices were transferred to the petri dish and maintained there for 3 h. The slices were then stored at room temperature in a holding saline comprised of the Calcium Orange loading saline and 2 ml of ACSF until 30 min before use, at which point they were stained with RH-414.

The RH-414 staining saline consisted of 3 ml of ACSF, 1 ml of the holding saline, and 10 μl of RH-414 stock (4 mM RH-414 in distilled water); the final concentrations were: 10 μM RH-414, 3.3 μM Calcium Orange-AM, 0.06% DMSO and 0.02% pluronic acid. A Calcium Orange-loaded slice was stained in this solution for 15 min at room temperature. Excess dye was removed by transferring the slice to approximately 10 ml of ACSF and washing for 15 min.

2.5. Recording

For recording, slices were transferred to a temperature-controlled (room temperature or 31–32°C) submersion chamber on the stage of the microscope. The perfusion rate was approximately 5 ml/min. A low-resistance (1–5 MΩ) glass microelectrode, filled with ACSF, was used to record the field potential as a control. For recording evoked responses, a bipolar tungsten stimulation electrode was placed in stratum radiatum of area CA1. Responses were evoked with 500 μsec current pulses delivered at frequencies less than 0.05 Hz; occasionally, paired pulses (50 ms interpulse interval) were used.

To obtain a record, first a measurement was made in DC-coupled mode (second stage gain = 1 or 10) to obtain the value for the static fluorescence (F), this was followed by a measurement in slow AC-coupled mode (second stage gain = 1000 or 5000) to obtain the fluorescence transient (ΔF). The shutter was pre-opened for 500 ms before each measurement to allow for settling of the PDAs. For evoked responses, stimuli were applied during the measurement period; for spontaneous events, the AC-coupled measurement was repeated at intervals longer than 10 s until a spontaneous event occurred during the measurement period.

2.6. Processing

All optical data are expressed as change in fluorescence over static fluorescence ($\Delta F/F$). This corrects for variations in dye concentration, in illumination intensity, and in the sensitivity of the detectors, assuming that these quantities do not change significantly during the course of measuring ΔF and F. The normalized quantity, $\Delta F/F$, is proportional to the change in calcium concentration or in membrane potential. Because we want to study the spread of evoked activity and SEA, we are interested in the spatio-temporal pattern of the transients of V_m and $[Ca^{2+}]_i$ rather than their absolute values. Therefore, we did not attempt to calibrate the optical signals.

As discussed previously, although the emission spectra of the 2 indicators are quite distinct, there is some overlap. Furthermore, the characteristics of the optical filters are such that perfect separation of the emission from the 2 indicators would not be obtained even if their spectra did not overlap. For these reasons, some cross-talk was expected between the signals recorded by the 2 PDMs. Assuming the normalized spectra of the dyes to be constant, i.e., only the amplitude, but not the shape, of the spectrum changes with calcium concentration or membrane potential, a simple correction procedure can be used which relies on forming a linear combination of the 2 signals (Carlsson and Mossberg, 1992):

$$\begin{bmatrix} S_1' \\ S_2' \end{bmatrix} = \begin{bmatrix} 1 & -\alpha_2 \\ -\alpha_1 & 1 \end{bmatrix} \begin{bmatrix} S_1 \\ S_2 \end{bmatrix} \quad (1)$$

where S_1 is the raw signal recorded by an element of PDM_1, S_1' is the corrected signal for that element; S_2 and S_2' are similarly defined for PDM_2. The proportionality factors, α_i, represent the amount of cross-talk for each detector: α_1 is the ratio of the fluorescence recorded in PDM_2 to that in PDM_1 when only dye 1 (Calcium Orange) is present; α_2 is the ratio of the fluorescence recorded in PDM_1 to that in PDM_2 when only dye 2 (RH-414) is present.

Lastly, optical signals were corrected for dye bleaching. To measure bleaching, optical signals were recorded during period when no stimulation was applied (for evoked activity) or during a period where no spontaneous activity was seen (for SEA). After correcting for crosstalk and calculating $\Delta F/F$ for both the bleaching and the actual recordings, the bleaching records were subtracted from the actual signals.

3. Results

Using the strategy, apparatus, and procedures described above, we were able to simultaneously record membrane potential and intracellular calcium transients from guinea pig hippocampal brain slices with high spatio-temporal resolution. The temporal resolution of the system is 570 μs; with a 10 × objective, the spatial resolution is 200 × 200 μm/element.

3.1. Dye loading

Calcium Orange-AM proved to be relatively difficult to load into slices. Relatively long incubation periods, increased temperatures, and a relatively high concentration of pluronic acid were required to load slices with Calcium Orange. Also, as noted by other researchers (Yuste and Katz, 1991), we noticed an inverse correlation between loading and the age of the guinea pigs; very poor loadings were obtained in slices from animals older than 2 weeks. Slices from older animals also tended to not retain the Calcium Orange as well after removal from the staining solutions. All slices showed some washout of Calcium Orange, although, in the younger animals, it was possible to record calcium transients for over 2 h at 31–32°C. Retention of Calcium Orange was greatly improved at room temperature.

In contrast to Calcium Orange-AM, RH-414 was very easy to load. In fact, we were able to use 10–20-fold lower concentrations than previously used (Colom and Saggau, 1994). Although a higher concentration of RH-414 would increase the quality of the VSD signal, we used a smaller concentration to minimize the amount of cross-talk into the Calcium Orange signal and the possible photodynamic damage caused by highly reactive molecules which may be generated from the VSD during light exposure. The small amount of pluronic acid present in the staining solution, greatly facilitated staining, probably by increasing the solubility and diffusion rate of RH-414 in the slice.

3.2. Light source

The relatively small fractional signals ($\Delta F/F$) we were measuring together with the low fluorescence obtained from Calcium Orange require a stable, high-intensity source of illumination. A battery-powered tungsten lamp, which our lab has used in the past to

record signals from RH-414 (Colom and Saggau, 1994), is very stable (< 0.01% peak-to-peak noise) but does not provide sufficient intensity to record the Calcium Orange signals. In contrast, a conventional xenon burner setup, which is approximately 400% more intense, is not stable enough for this application. By running a xenon burner from a constant current source whose power supply is buffered with batteries, we were able to obtain a relatively stable (< 0.05% peak-to-peak noise), high-intensity illumination.

3.3. Cross-Talk

The proportionality factors, α_1 and α_2, in Eq. 1 were measured using slices stained with only 1 of the 2 indicators. When only RH-414 (dye 2 in Eq. 1) was present, the fluorescence recorded in PDM_1 was 14.1% of that recorded by PDM_2; α_2 had a value of 0.141. When only Calcium Orange (dye 1) was present, the fluorescence in PDM_2 was less than the detected noise, indicating that the amount of cross-talk was too small to be measured; therefore, a value of zero was used for α_1. Fig. 4 shows that using these values with the correction procedure described by Eq. 1 was effective in removing the cross-talk between the 2 indicators. This procedure was applied to all data.

3.4. Transients associated with evoked activity

Evoked activity was recorded in both area CA1 and CA3 of the hippocampal slice. In Fig. 4B, the 3 main components of the field potential in area CA1 can be clearly distinguished: a fiber volley representing the action potential in the stimulated presynaptic fibers, a field excitatory postsynaptic potential (fEPSP), and a population spike representing the firing of the postsynaptic CA1 pyramidal cells. All 3 of these components can also be clearly seen in the optically recorded membrane potential transient. The differences between the field potential and the optically recorded membrane

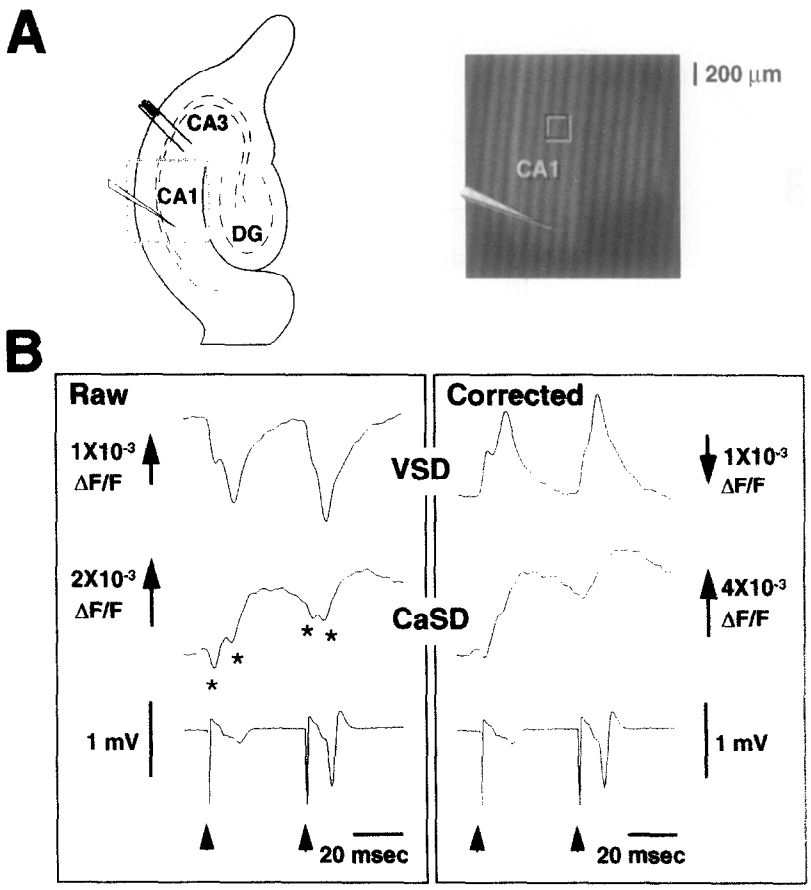

Fig. 4. Data processing and cross-talk correction. Transients of V_m (VSD signal) and $[Ca^{2+}]_i$ (CaSD) evoked by 2 stimuli (50 ms apart) delivered to stratum radiatum of CA1 were recorded in area CA1. A: schematic of a hippocampal slice is shown on the left. The square represents the area covered by the PDM; the positions of the stimulation and recording electrode are indicated. An CCD image of the recording area is shown to the right; the black square represents the single PDM element from which the data is shown. B: the field potential, recorded at the position indicated by the microelectrode on the image, is shown at the bottom under both the raw and the corrected data; the arrows below the field potential indicate the time of stimulation. The raw optical signals (VSD on top) are shown on the left; the corrected signals are on the right. For V_m, the only correction was to invert the signal so that an upward deflection in the optical trace corresponds to depolarization. In the raw $[Ca^{2+}]_i$ transient (CaSD in the middle), clear downward humps (*) due to crosstalk from the VSD signal are apparent. The correction procedure described by Eq. 1 was applied to obtain the corrected signal shown on the right. The responses shown are an average of 4 trials.

potential transient are partially due to the difference between the quantities measured by the 2 methods. The field potential reflects the extracellular field due to activation of neurons. Its polarity depends on the relative location of the electrode to the current sources and sinks and whether these are active or passive. The time course of the field potential is approximately that of the transmembrane current (for review see: Johnston and Wu, 1995). In contrast, the optical signal is the weighted average of the transmembrane potentials of all stained structures covered by a single photodiode. The weight depends on the number of dye molecules bound to the plasma membrane of the neural structure, which is proportional to the membrane area. With the VSD RH-414, all depolarizations will be seen as a decrease in fluorescence and all hyperpolarizations as an increase. The longer time course of the optical signal compared to field potential is probably due to the fact that the time course of the optical signal is the same as that of the membrane potential, whereas the time course of the field potential is that of the transmembrane current. Another factor is that, at this spatial resolution, the optical signal probably records from a larger group of neurons then the field potential. This would predict that the observed time course of the optical signals will be shorter with a higher magnification objective (higher spatial resolution). Indeed, shorter time courses were obtained with a 40 × objective (Sinha and Saggau, unpublished observation).

The effect of blocking excitatory synaptic transmission in area CA1 by bath applying the ionotropic glutamate receptor antagonists, CNQX (10 μM) and D-APV (50 μM), is shown in Fig. 5. This manipulation

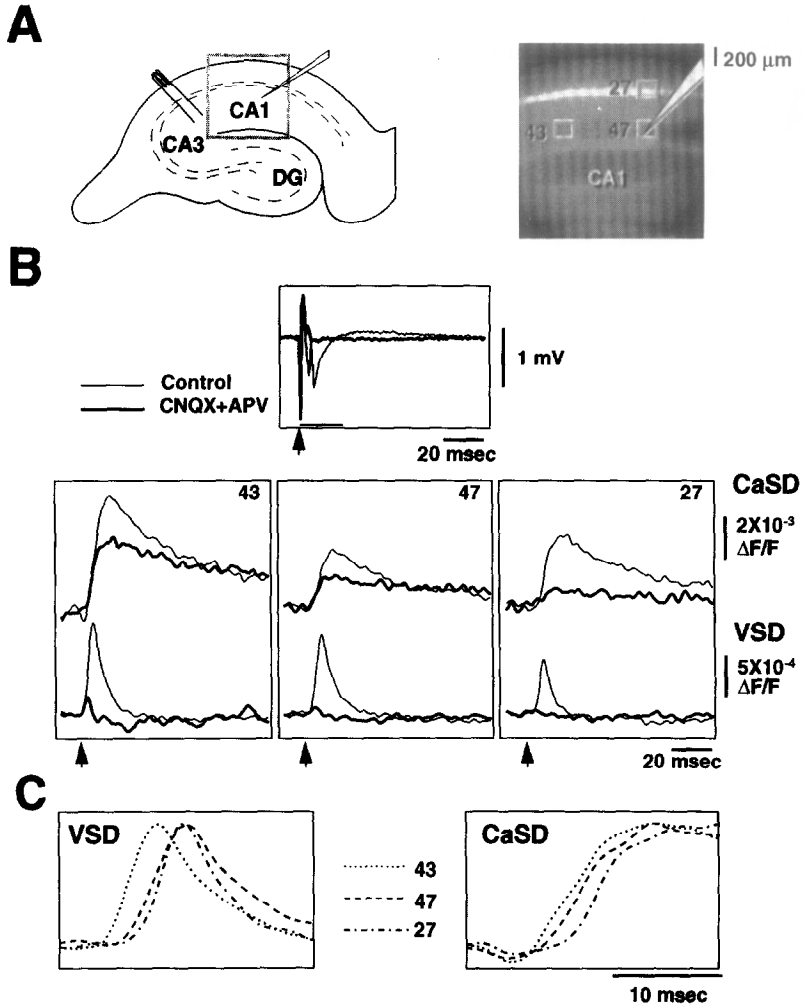

Fig. 5. Evoked activity in area CA1. A: schematic of the slice, including recording area and locations of stimulation and recording electrode, is shown at the left. The image of the recording area is shown at the right; the numbered black squares indicate the PDM elements from which data is shown at the bottom. B: responses were evoked by a single stimulus delivered to stratum radiatum of area CA1. The field potential recorded at the point indicated by the electrode is shown on the top; the arrow indicates the time of stimulation and the horizontal bar indicates the time window shown on an expanded time scale in (C). The thin traces correspond to control conditions; the thick traces were recorded in the presence of the glutamate antagonists CNQX (10 μM) and D-APV (50 μM). The optical signals from the numbered PDM elements are shown at the bottom, CaSD in the top row, VSD in the bottom row. Again, the arrow indicates the time of stimulation. C: normalized control optical responses from (B) are shown on an expanded time scale, VSD on the left and CaSD on the right.

reduced the field potential and optically recorded voltage transient to the afferent fiber volley (Fig. 5B). The fiber volley did not change. The calcium transient was differently affected in different areas of the slice: it was almost abolished in stratum pyramidale, which consists largely of the cell bodies of the postsynaptic CA1 pyramidal cells, but was much less affected in stratum radiatum, the location of the presynaptic terminals and postsynaptic dendrites. Typically, the calcium transient was reduced by 20–30%, indicating that under control conditions, the calcium transient is largely a reflection of calcium influx into presynaptic structures.

The spatio-temporal variation of the optical signals is shown in Fig. 5C. In the VSD signals, the propagation of the evoked activity can be clearly seen: activity traveled along the stimulated axons from the site of stimulation across stratum radiatum. Comparing the signal in channel 43 and that in 47, whose centers are separated by 800 μm, a delay of 1–2 ms is apparent; this leads to an estimate of 400–800 mm/s for the conduction velocity of the CA3 pyramidal cell axons. Propagation of the postsynaptic response along the dendritic tree of the CA1 pyramidal cells can also be detected; for example, the response recorded in channel 47 (dendritic area) and that in channel 27 (cell body layer). Activity occurred first in the dendritic area, representing the presynaptic action potential and local postsynaptic response, and spread to the cell body layer. Note, however, the activity seemed to peak first in the cell body layer. This may be because the peak correlates with the postsynaptic action potentials which originate in or near the cell body layer and then spread back into the dendrites.

The calcium transients always started after the corresponding voltage transient (Fig. 5A). This is a reflection of the fact that most of the calcium influx is through voltage-dependent calcium channels, which require depolarization to open, and also of the slower kinetics of the CaSD compared to the VSD. Spatial variation can also be seen in the CaSD signals. In stratum radiatum, where the calcium transient contains mainly presynaptic but also some postsynaptic components, the spread of the transient away from the stimulation site is apparent (channels 43 and 47). The calcium transient in the cell body layer (channel 27), which is mostly postsynaptic, occurs after the transient in the corresponding dendritic area.

In area CA3 (Fig. 6), the field potential recorded in

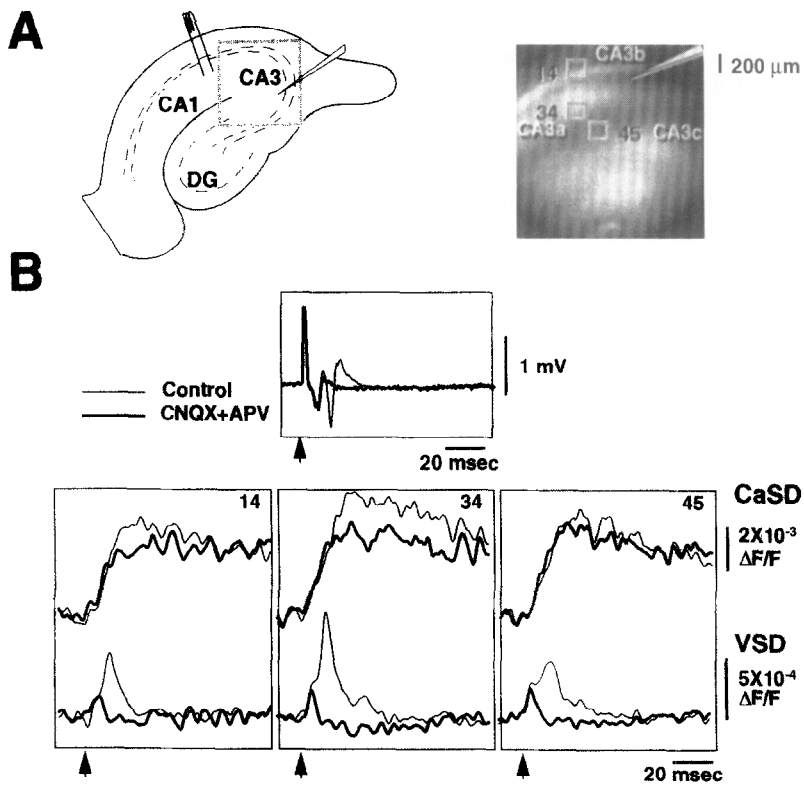

Fig. 6. Evoked activity in area CA3. A: schematic of the slice, including recording area and locations of stimulation and recording electrode, is shown at the left. The recording area is shown at the right; the numbered black squares indicate the PDM elements from which data is shown. B: responses were evoked by a stimulus delivered to stratum radiatum of area CA1, which antidromically activated the area CA3 pyramidal cells. The field potential recorded at the point indicated by the microelectrode is at the top; the arrow indicates the time of stimulation. The thin traces correspond to control conditions; the thick traces were recorded in the presence of CNQX (10 μM) and D-APV (50 μM). The optical signals from the numbered PDM elements are shown at the bottom, CaSD in the top row, VSD in the bottom row. The arrow indicates the time of stimulation.

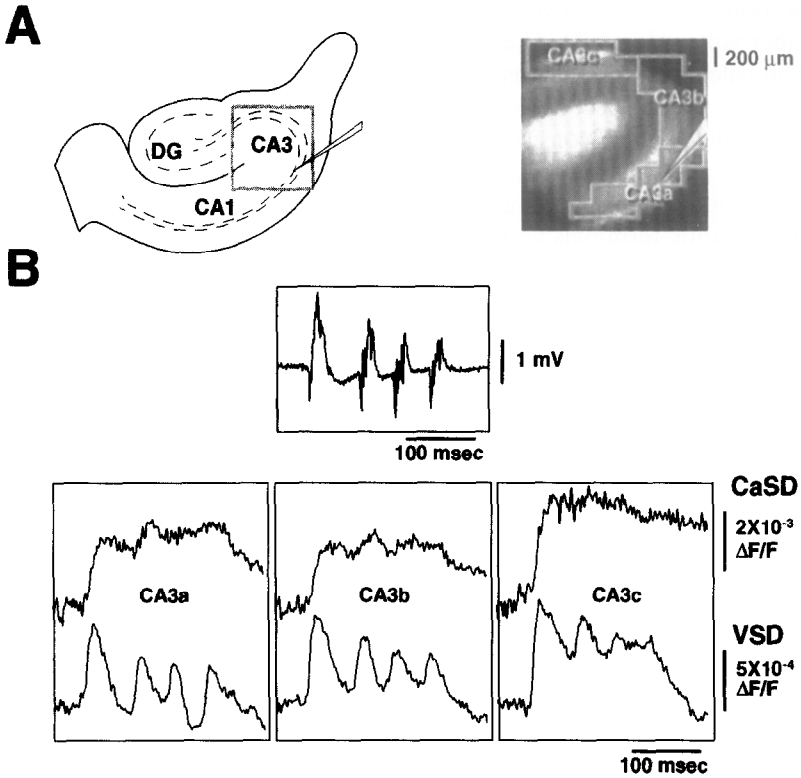

Fig. 7. Spontaneous epileptiform activity in area CA3. Spontaneous epileptiform activity was induced by bath application of 100 μM 4-aminopyridine. A: schematic of the slice, indicating the recording area and the location of the recording electrode, is shown on the left. The recording area is shown at the right. For purposes of display, area CA3 was subdivided into 3 equal-sized sub-areas: CA3a, CA3b and CA3c. B: the field potential recorded at the point indicated by the microelectrode is shown at the top. The data from all PDM elements within a sub-area were binned together. The binned optical signals from the 3 sub-areas are shown at the bottom, CaSD in the top row, VSD in the bottom row. Analysis of the VSD signals indicates that this epileptiform discharge originated in sub-area CA3c. The responses were digitally filtered to remove residual line noise.

response to antidromic activation of CA3 pyramidal cells consisted of the directly evoked action potential, followed by a fEPSP and population spike due to activation of recurrent excitatory connections between the pyramidal cells. Application of CNQX (10 μM) and D-APV (50 μM), reduced the field potential and the optically recorded membrane potential to the directly evoked action potential. The amplitude of the calcium transient was also reduced; however, no conclusions can be drawn about the relative contribution of pre- and postsynaptic components because the antidromic stimulus can activate both the dendrites and the recurrent axons even when synaptic transmission is blocked.

3.5. Transients associated with SEA

In order to test the ability of the recording system to detect spontaneous neural activity, we applied the potassium channel blocker 4-aminopyridine (100 μM). Three possible mechanisms (for discussion, see Colom and Saggau, 1994) by which 4-AP could produce SEA are: (1) a reduction of outward potassium currents leading to a depolarization of neurons; (2) an increase in neurotransmitter release; or (3) a decrease in the efficacy of GABA-mediated inhibition due to a shift in the chloride equilibrium potential. At 32°C, SEA appeared within 5 min of 4-AP application. An event along with the associated membrane potential and intracellular calcium transients is shown in Fig. 7. The onset of the VSD signal could be used to establish the site of origin of the spontaneous event (Colom and Saggau, 1994).

4. Discussion

The strategy, techniques, and equipment described here allow simultaneous recording of membrane potential and calcium transients with high spatio-temporal resolution with sufficient sensitivity to record spontaneous as well as evoked activity, i.e., without the need for averaging several responses.

The use of the technique of bulk loading by bath application of the indicators raises a question as to the nature of the signals recorded. Previous work in our laboratory and by others has indicated that the membrane potential transients obtained with RH-414 are neuronal rather than glial in origin (for review see Salzberg, 1989). The relatively fast time courses of both

transients also argue in favor of a neuronal origin. The signals measured were from both presynaptic and postsynaptic structures. The temporal aspects of the signal and, in some cases, pharmacological tools can be used to separate presynaptic and postsynaptic signals. For example, the use of CNQX and D-APV allows the measurement of an isolated presynaptic calcium transient in area CA1.

For the calcium indicator, loading techniques using either local perfusion of the indicator (Regehr and Tank, 1991) or localized pressure application (Wu and Saggau, 1994) could be used to selectively load structures in hippocampal slices, such as presynaptic structures in CA1, postsynaptic structures in CA1, or mossy fiber tracts in CA3. However, the relatively low fluorescence levels achieved by these techniques would probably prohibit the use of a photodiode array or any other detector with spatial resolution without the need for substantial temporal integration and/or averaging. Other selective loading techniques may be available for use with other preparation; for example, uptake of membrane-impermeant forms of calcium indicators by lesioned nerve roots of the spinal cord (O'Donovan et al., 1993).

The technique described here for simultaneous recording of signals from 2 optical indicators can be generalized for use with any 2 or more indicators that have overlapping excitation and separable emission spectra. These spectra should be such that filters and dichroic mirrors can be found which allow for obtaining signals with no cross-talk. Due to the relatively close spacing of the emission spectra of indicators which have overlapping excitation spectra and the nature of available filters and dichroic mirrors (see Section 2.6), some cross-talk should be expected for any combination of such indicators. In order to be able to correct for this cross-talk, it is necessary that the normalized spectra of the dyes be constant, i.e., the shapes of the spectra should not change. This constraint rules out the use of all dual wavelength (ratiometric) dyes. To our knowledge, Calcium Orange and RH-414 are the only indicators which meet all these requirements to date; however, matched pairs of indicators could be synthesized for use with this technique.

Several modifications could be made to the hardware described here to suit particular applications. Better spatial resolution could be obtained with a higher magnification objective at the cost of reducing the overall size of the recording area; covering a larger recording area by using a lower magnification objective would be difficult due to the lower numerical aperture (NA) of low-magnification objectives, which leads to a lower light-gathering capability (Saggau, 1994). Spatial resolution could also be improved by using either CCDs or PDMs with more elements; however, this would mean sacrificing temporal resolution. For CCDs, even with special modifications, the best temporal resolution is on the order of 100 frames/s (for 18×18 elements, Lasser-Ross et al., 1991) and the sensitivity to light is such that temporal integration and/or averaging is usually necessary. Although large PDMs can provide good temporal resolution, due to the smaller size of individual elements, the fluorescence intensity seen by each element may be too low to obtain signals without considerable averaging. (Note: most studies using large PDMs utilize absorption measurements which give higher light intensities at the detector.) Temporal resolution and sensitivity could be improved significantly at the cost of spatial resolution by using single photodiodes. The size and location of the recording area could then be controlled by apertures placed in the light pathway. With these limitations in mind, various combination of detectors could be used with this strategy depending on the spatial and temporal resolutions and sensitivity required.

The temporal resolution of the system could also easily be improved by using a faster A/D card, which is readily available (for example: 1 MHz sampling rate, DAS 50, MetraByte, Taunton, MA). The resolution could be further improved if, instead of recording the signal from every element of the photodiode array, only signals from selected elements of interest were recorded. To implement this, an approach we are taking in our laboratory is to use a digital I/O card with on-board memory; the addresses of the user-selected PDM elements are stored in the memory and output to the multiplexer (Cakir, 1993). The increase in temporal resolution will be inversely proportional to the fraction of matrix elements selected for recording.

Finally, the recording procedure could be simplified if a 16-bit A/D card was used instead of the 12-bit. With the higher dynamic range offered by the 16-bit A/D card, all data could be collected in DC-coupling mode; currently, we have to switch between a low-gain DC-coupling (to record static fluorescence) and a higher-gain AC-coupling mode (to record transients). Another improvement would be the addition of a reference diode to measure noise in the excitation light in order to correct for noise in the illumination (Cakir, 1993).

In summary, we have developed a novel strategy, based on the opportune characteristics of 2 indicators, for simultaneous recording of membrane potential and calcium transients. Our implementation of this strategy provides for recording these transients with high spatio-temporal resolution (200×200 μm and 570 μs, respectively) for both evoked and spontaneous events in brain slices. We have also discussed possible modifications to the loading methods and the detector which may be used depending on the particular requirements of the application. Lastly, hardware improvements to the current system were discussed.

Acknowledgements

We thank Drs. R. Gray, D. Johnston and W. Schilling for kindly allowing us to use some of their equipment, and A. Bullen and Drs. B. Christie and L.-G. Wu for critical and helpful comments on the manuscript. This work was supported by an NRSA predoctoral fellowship from NIMH to S.R.S. and by departmental funds.

References

Albowitz, B., Kuhnt, U. and Ehrenreich, L. (1990) Optical recording of epileptiform voltage changes in the neocortical slice, Exp. Brain Res., 81: 241–256.

Cakir, H.C. (1993) Development of a Computer-Based Control System for a Confocal Laser Scanning Microscope. University of Houston, Houston, TX.

Carlsson, K. and Mossberg, K. (1992) Reduction of cross-talk between fluorescent labels in scanning laser microscopy, J. Microsc., 16: 23–37.

Cinelli, A.R. and Kauer, J.S. (1992) Voltage-sensitive dyes and functional activity in the olfactory pathway, Ann. Rev. Neurosci., 15: 321–351.

Colom, L.V. and Saggau, P. (1994) Spontaneous interictal-like activity originates in multiple areas of the CA2-CA3 region of hippocampal slices, J. Neurophys., 71: 1574–1585.

Fromherz, P. and Vetter, T. (1992) Cable properties of arborized retzius cells of the leech in culture as probed by a voltage-sensitive dye, Proc. Natl. Acad. Sci. USA, 89: 2041–2045.

Fukunishi, K., Murai, N. and Uno, H. (1992) Dynamic characteristics of the auditory cortex of guinea pigs observed with multichannel optical recording, Biol. Cyber., 67: 501–509.

Grinvald, A., Cohen, L.B., Lesher, S. and Boyle, M.B. (1981) Simultaneous optical monitoring of activity of many neurons in invertebrate ganglia using a 124-element photodiode array, J. Neurophys., 45: 829–840.

Haugland, R.P. (1992) Handbook of Fluorescent Probes and Research Chemicals, 5th edn., Molecular Probes, Eugene, OR, 421 pp.

Hess, G. and Kuhnt, U. (1992) Presynaptic calcium transients evoked by paired pulse stimulation in the hippocampal slice, NeuroReport, 3: 361–364.

Johnston, D. and Wu, S. (1995) Foundations of Cellular Neurophysiology, MIT Press, Cambridge, MA.

Kremer, S.G., Zeng, W. and Skorecki, K.L. (1992) Simultaneous fluorescence measurement of calcium and membrane potential responses to endothelin, Am. J. Physiol., 263: C1302–C1309.

Lasser-Ross, N., Miyakawa, H., Lev-Ram, V., Young, S.R. and Ross, W.N. (1991) High time resolution fluorescence imaging with a CCD camera, J. Neurosci. Methods, 36: 253–261.

Litaudon, P., and Cattarelli, M. (1992) Origin of the in vivo rat piriform cortex activity recorded with voltage-sensitive dyes: comparison of the optical signals and the field potentials, Brain Res., 594: 171–175.

Martinez-Zaguilan, R., Martinez, G.M., Latanzio, F. and Gillies, R.J. (1991) Simultaneous measurements of intracellular pH and Ca^{2+} using the fluorescence of SNARF-1 and fura-2, Am. J. Physiol., 260: C297–C307.

Miyata, H., Hayashi, H., Suzuki, S., Noda, N., Kobayshi, A., Fujiwake, H., Hirano, M. and Yamazaki, N. (1989) Dual loading of the fluorescent indicator fura-2 and 2,7-biscarboxyethyl-5(6)-carboxyfluorescein (BCECF) in isolated myocytes, Biochem. Biophys. Res. Comm., 163: 500–505.

Montana, V., Farkas, D.L. and Loew, L.M. (1989) Dual-wavelength ratiometric fluorescence measurements of membrane potential, Biochemistry, 28: 4536–4539.

Morris, S.J. (1992) Simultaneous multiple detection of fluorescent molecules: rapid kinetic imaging of calcium and pH in living cells. In: B. Herman and J.J. Lemasters (Eds.), Optical Microscopy: New Technologies and Applications, Academic Press, New York.

Murphy, T.H., Baraban, J.M., Wier, W.G. and Blatter, L.A. (1994) Visualization of quantal synaptic transmission by dendritic calcium imaging, Science, 263: 529–532.

O'Donovan, M.J., Ho, S., Sholomenko, G. and Yee, W. (1993) Real-time imaging of neurons retrogradely and anterogradely labelled with calcium-sensitive dyes, J. Neurosci. Methods, 46: 91–106.

Patel, S.S., Colom, L.V. and Saggau, P. (1993) Optical imaging of carbachol-induced spontaneous epileptiform oscillations in guinea pig hippocampal brain slices. Soc. Neurosci. Abst., 19: 420.19.

Regehr, W.G. and Tank, D.W. (1991) Selective fura-2 loading of presynaptic terminals and nerve cell processes by local perfusion of mammalian brain slice, J. Neurosci. Methods, 37: 111–119.

Ross, W.N., Arechiga, H. and Nicholls, J.G. (1988) Influence of substrate on the distribution of calcium channels in identified leech neurons in culture, Proc. Natl. Acad. Sci. USA, 85: 4075–4078.

Saggau, P., Galvan, M. and Tenbruggencate, G. (1986) Long-term potentiation in guinea pig hippocampal slices monitored by optical recording of neuronal activity, Neurosci. Lett., 69: 53–58.

Saggau, P. and Tenbruggencate, G. (1988) Topology related real-time monitoring of neural activity in hippocampal brain slices by noninvasive optical recording: a step towards functional aspects of long-term potentiation (LTP). In: H.L. Haas and G. Buszaki (Eds.), Synaptic Plasticity of the Hippocampus, Springer, Berlin, pp. 159–162.

Saggau, P. and Sheridan, R.D. (1990) Fast transients of membrane potential and cytosolic calcium in guinea pig hippocampal brain slices. In: R. Flores and J. Louvel (Eds.), Optical Recording of Transmembrane Potential in Excitable Cells, Le Vesignet, Paris.

Saggau, P. (1994) Optical recording from neural populations in vitro: application of laser scanning microscopy. In: D.A. Stenger and T.M. McKenna (Eds.), Enabling Technologies for Cultured Neural Networks, Academic Press, New York, pp. 187–205.

Salzberg, B.M. (1989) Optical recording of voltage changes in nerve terminals and in fine neuronal processes, Ann. Rev. Physiol., 51: 507–526.

Tepikin, A.V., Voronina, S.G., Gallacher, D.V. and Petersen, O.H. (1992) Acetylcholine-evoked increase in the cytoplasmic Ca^{2+} concentration and Ca^{2+} extrusion measured simultaneously in single mouse pancreatic acinar cells, J. Biol. Chem., 267: 3569–3572.

Yuste, R. and Katz, L.C. (1991) Control of postsynaptic Ca^{2+} influx in developing neocortex by excitatory and inhibitory neurotransmitters, Neuron, 6: 333–344.

Wu, L.G. and Saggau, P. (1994) Presynaptic calcium is increased during normal synaptic transmission and paired-pulse facilitation, but not in long-term potentiation in area CA1 of hippocampus, J. Neurosci., 14: 645–654.

Zorec, R., Hoyland, J. and Mason, W.T. (1993) Simultaneous measurements of cytosolic pH and calcium interactions in bovine lactotrophs using optical probes and four-wavelength quantitative video microscopy, Pflugers. Arch., 423: 41–50.